Langmuir Article

pubs.acs.org/Langmuir

Capillary Condensation and Evaporation in Alumina Nanopores with Controlled Modulations

Lorenzo Bruschi,[†] Giampaolo Mistura,*[,†] Lifeng Liu,[‡] Woo Lee,[§] Ulrich Gösele,[‡,#] and Benoit Coasne*[,⊥]

[†]*Dipartimento di Fisica G.Galilei and CNISM, Università di Padova, via Marzolo 8, 35131 Padova, Italy,*
[‡]*Max Planck Institute for Microstructure Physics Weinberg 2, 06120 Halle, Germany,*
[§]*Korea Research Institute of Standards and Science (KRISS), Yuseong, 305-340 Daejon, Korea, and*
[⊥]*Institut Charles Gerhardt Montpellier, University Montpellier 2 and CNRS (UMR 5253), Montpellier, France*

Received March 19, 2010. Revised Manuscript Received May 7, 2010

Capillary condensation in nanoporous anodic aluminum oxide presenting not interconnected pores with controlled modulations is studied using adsorption experiments and molecular simulations. Both the experimental and simulation data show that capillary condensation and evaporation are driven by the smallest size of the nanopore (constriction). The adsorption isotherms for the open and closed pores are almost identical if constrictions are added to the system. The latter result implies that the type of pore ending does not matter in modulated pores. Thus, the presence of hysteresis loops observed in adsorption isotherms measured in straight nanopores with closed bottom ends can be explained in terms of geometrical inhomogeneities along the pore axis. More generally, these results provide a general picture of capillary condensation and evaporation in constricted or modulated pores that can be used for the interpretation of adsorption in disordered porous materials.

Introduction

Capillary condensation of molecular fluids in nanoporous materials is of fundamental interest in understanding the effect of confinement and surface forces on the thermodynamics and dynamics of fluids.[1−5] From a practical viewpoint, adsorption of fluids in nanopores is also relevant to practical applications in the field of catalysis, oil extraction, mixture separation, pollution control, etc. Capillary condensation in nanoporous materials is usually an irreversible phenomenon, as revealed by significant and reproducible hysteresis loops observed during adsorption/desorption cycles.[1,6] This hysteretic behavior, which is common both to nanoporous materials with not interconnected pores and to ordinary porous glasses like Vycor and aerogel characterized by a complex network of connected pores, is often explained using one of the following models. Hysteresis loops observed for not interconnected pores of a simple regular geometry are usually interpreted as a change in the symmetry of the gas/liquid interface upon filling and emptying.[7] In contrast, in the case of connected or irregular pores, the hysteresis loop is ascribed to the existence of constrictions or bottlenecks between pores that cause a delay in the desorption process compared to the adsorption.[8]

While the nature of capillary condensation hysteresis for individual pores of a simple geometry has been clarified,[9−11] the status of the vapor/liquid phase transition for disordered pores (i.e., irregular individual pores and complex disordered network of pores) remains puzzling. Experimental,[12] theoretical,[13] and molecular simulation[14] works have shown that morphological defects such as constrictions affect the pore filling and emptying mechanisms. Depending on system parameters, the emptying of the pores is triggered either by pore blocking (the liquid remains trapped in the large pore sections until it first desorbs from the pore constrictions) or cavitation (the liquid trapped in the pores desorbs through the spontaneous nucleation of a gas bubble). The situation for irregular pores is even more puzzling as recent calculations suggest that capillary condensation hysteresis for disordered porous materials such as Vycor is due to the complexity of the free energy landscape with a very large number of metastable states in which the fluid remains trapped.[15] Recent experiments and molecular simulations have also shown that the dynamics of the confined fluid within the hysteresis region is drastically slowed down as it corresponds to density rearrangements of the adsorbate in the porosity of the host material.[4,16,17] Finally, the interpretation of the experiments is often complicated by the fact that real porous materials generally present various sources of disorder including irregularities in pore size, roughness of surface walls, chemical heterogeneities, pore openings, and three-dimensional pore connectivity, whose effects are difficult to deconvolve.

*Corresponding authors. E-mail: mistura@padova.infm.it (G.M.); benoit.coasne@enscm.fr (B.C.).
[#]Deceased Nov 8, 2009.

(1) Gelb, L. D.; Gubbins, K. E.; Radhakrishnan, R.; Sliwinska-Bartkowiak, M. *Rep. Prog. Phys.* **1999**, *62*, 1573–1659.
(2) Coasne, B.; Grosman, A.; Ortega, C. *Phys. Rev. Lett.* **2002**, *88*, 256102.
(3) Wallacher, D.; Kunzner, N.; Kovalev, D.; Knorr, N.; Knorr, K. *Phys. Rev. Lett.* **2004**, *92*, 195704.
(4) Valiullin, R.; Naumov, S.; Galvosas, P.; Karger, J.; Woo, H. J.; Porcheron, F.; Monson, P. A. *Nature* **2006**, *443*, 965–968.
(5) Gunther, G.; Prass, J.; Paris, O.; Schoen, M. *Phys. Rev. Lett.* **2008**, *101*, 086104.
(6) Bruschi, L.; Mistura, G. *J. Low Temp. Phys.* **2009**, *157*, 206–220.
(7) Cohan, L. H. *J. Am. Chem. Soc.* **1938**, *60*, 433–435.
(8) Everett, D. H. In *The Structure and Properties of Porous Materials*; Everett, D. H., Stone, F. S., Eds.; Butterworths: London, 1958; p 95.
(9) Evans, R.; Marini Bettolo Marconi, U.; Tarazona, P. *J. Chem. Soc., Faraday Trans.* **1986**, *82*, 1763.
(10) Sarkisov, L.; Monson, P. A. *Langmuir* **2001**, *17*, 7600.
(11) Gelb, L. D. *Mol. Phys.* **2002**, *100*, 2049.
(12) Thommes, M.; Smarsly, B.; Groenewolt, M.; Ravikovitch, P. I.; Neimark, A. V. *Langmuir* **2006**, *22*, 756–764.
(13) Vishnyakov, A.; Neimark, A. V. *Langmuir* **2003**, *19*, 3240–3247.
(14) Coasne, B.; Galarneau, A.; Di Renzo, F.; Pellenq, R. J. M. *J. Phys. Chem. C* **2007**, *111*, 15759–15770.
(15) Kierlik, E.; Monson, P. A.; Rosinberg, M. L.; Sarkisov, L.; Tarjus, G. *Phys. Rev. Lett.* **2001**, *87*, 055701.
(16) Naumov, S.; Valiullin, R.; Karger, J.; Monson, P. A. *Phys. Rev. E* **2009**, *80*, 031607.
(17) Naumov, S.; Khokhlov, A.; Valiullin, R.; Karger, J.; Monson, P. A. *Phys. Rev. E* **2008**, *78*, 060601.

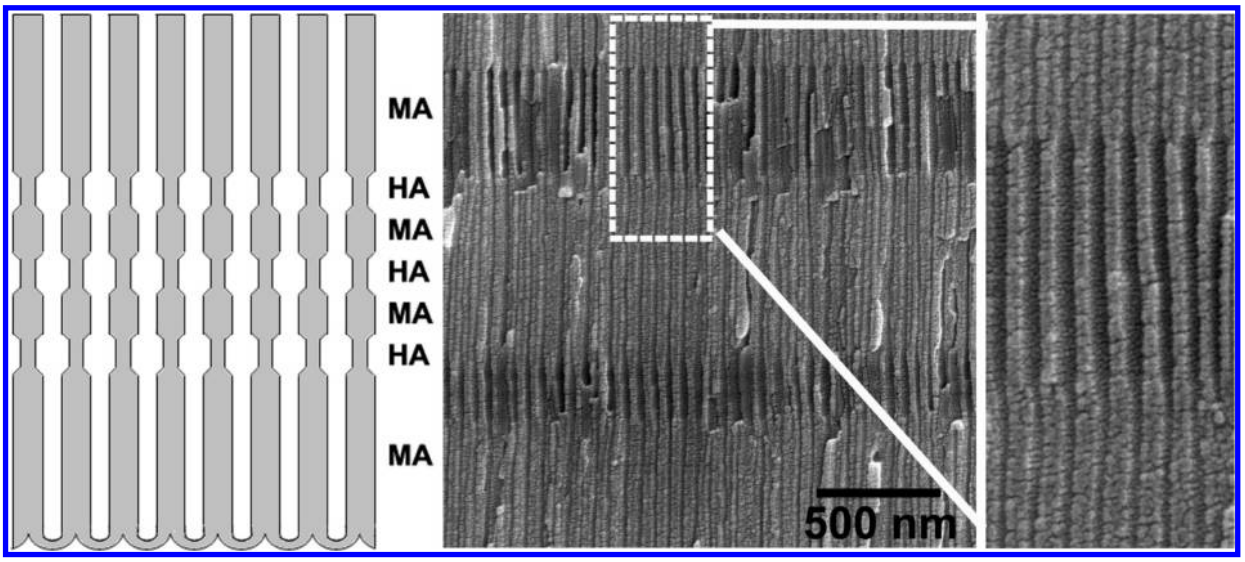

Figure 1. (left) Schematic diagram of a closed bottom modulated pore with $N = 3$. (right) Cross-section micrograph of the AAO membrane showing the modulations in pore diameter and an enlarged view of them.

This motivates the need for experiments and molecular simulations in nanoporous materials in which the disorder can be somewhat controlled. Porous anodized aluminum oxide (AAO) provides a good realization of such materials as it exhibits a collection of relatively smooth, not interconnected pores which can be prepared with controlled modulations. This contrasts with the very wide pore size distribution functions found in porous silicon[16] or the interconnections between individual channels in mesoporous silica SBA-15. Moreover, AAO nanopores can be prepared with pores closed at one end or open at both ends and then allow to test the effect of the pore extremity on the filling and emptying mechanisms. In the following, we report experiments and molecular simulations for argon adsorption in AAO nanopores of a simple cylindrical geometry but with a diameter D that varies in a controlled way along the pore axis (modulations). After a brief description of the experimental and molecular simulation techniques employed in this study, we present and comment on the main results of our work. We conclude by emphasizing that porous AAO is an ideal model substrate to investigate fluid adsorption in confined geometries.

Methods

Experiment. Both samples with the hemispherical barrier oxide layer at the pore bottoms (pores closed at one end) and samples without barrier oxide layer (pores opened at both ends) were prepared by a pulsed anodization method.[18] In brief, a high-purity Al foil (99.999%, Goodfellow) was first electropolished with a mixture of $HClO_4$ and C_2H_5OH (v/v 1:4) to obtain a mirror-like surface. Subsequently, the Al foil was subject to mild anodization in 0.3 M H_2SO_4 at 1 °C for 20 h, under a voltage of 25 V. The anodized Al foil was then immersed into a mixed solution of 1.8 wt % CrO_3 and 5 wt % H_3PO_4 at 45 °C for 20 h to remove the oxidized layer. Next, the textured Al foil was anodized under the same conditions as the first anodization for 7 h, and then a given number of potential pulses switching between 25 V (mild anodization, MA, 180 s) and 35 V (hard anodization, HA, 0.5 s) were introduced to create pore diameter modulations. After this, the Al foil was subject to MA again for 7 h. The pore diameter of the mild anodized parts is around 25 nm, while the pore diameter of the hard anodized parts is about 35 nm.

To obtain free-standing AAO membranes with closed bottom ends, the underlying Al substrate was selectively etched away. For preparing through-hole AAOs, the barrier layer was further removed. In this way, porous AAO with modulated pores open at both ends (O pores) or with closed bottom ends (C pores), having a total length of 100 μm and a variable number of large domains $N = 3$, 10, and 20 alternated by narrow ones, were prepared. Figure 1 shows the schematic structure of C pores for the case $N = 3$. The modulations in pore diameter are clearly visible in the enlargement of the cross section of the AAO membrane as examined by scanning electron microscopy displayed in Figure 1.

The AAO samples were disks ($D \sim 1$ cm) cut out of aluminum foils or alumina membranes with thickness of 400 and 100 μm, respectively. They were attached to the extremity of the tungsten rod of a torsional microbalance.[19] As the sample is exposed to a vapor, the resonance frequency decreases because of an increase in the total moment of inertia. This is caused by the mass of the adsorbed film and by the hydrodynamic contribution due to the mass of the dynamically displaced fluid. This latter contribution can be easily accounted for in the data analysis.[20] From the vapor corrected frequency shifts, it is then possible to derive the relative change of the oscillator moment of inertia which is proportional only to the mass of the adsorbed film.

Monte Carlo Simulations. In order to shed light on the experiments reported in the present work, we also performed grand canonical Monte Carlo simulations of argon adsorption at 85 K in models of cylindrical AAO pores with controlled morphologies. As with the experiments, we considered both samples open at both ends and closed at one end. The pore models were obtained by carving out of a block of amorphous alumina the desired porous materials. Two models were considered: regular cylindrical pores of different sizes ($D = 4.8$ nm and $D = 6.4$ nm and the same pore length $L = 25.6$ nm) and cylindrical nanopores with constrictions (main cylindrical channel with $D = 6.4$ nm and $L = 42.6$ nm modulated with two constrictions of $D_c = 4.8$ nm and $L = 14$ nm). All the pores are of a finite length and are open toward an external bulk reservoir, so that they mimic real materials for which the confined fluid is always in contact with the external gas phase. The pore sizes considered in the simulations are much smaller than those of the experimental samples to keep the number of argon atoms in the system reasonable ($< 10^5$). Nevertheless, the ratio $D/D_c = 2/3$ was chosen to correspond to that of the experimental samples. Argon was described as a Lennard-Jones (LJ) sphere with $\sigma = 3.405$ Å and $\varepsilon = 120$ K. The LJ parameters for the oxygen atoms of the alumina substrate are

(18) Lee, W.; Schwirn, K.; Steinhart, M.; Pippel, E.; Scholz, R.; Gosele, U. *Nature Nanotechnol.* **2008**, *3*, 234.

(19) Bruschi, L.; Carlin, A.; Mistura, G. *Phys. Rev. Lett.* **2002**, *89*, 166101.

(20) Bruschi, L.; Carlin, A.; Parry, A. O.; Mistura, G. *Phys. Rev. E* **2003**, *68*, 021606.

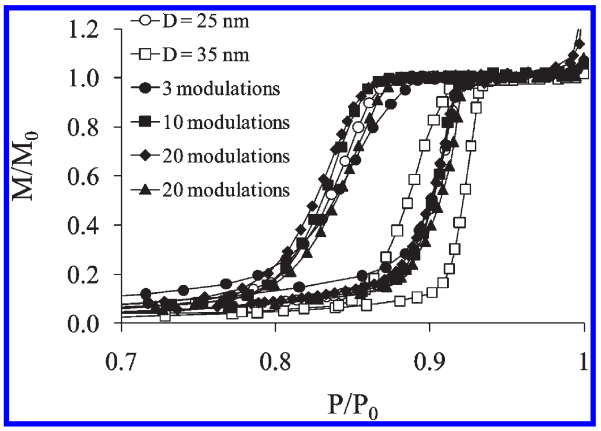

Figure 2. Experimental Ar adsorption isotherms at 85 K in porous AAO with straight and modulated pores closed at one end. Open symbols refer to straight pores with different nominal diameter D. Full symbols indicate modulated pores having a different number N of large domains (D = 35 nm) alternated by narrow ones (D = 25 nm). For the geometry N = 20, two isotherms are shown which refer to two different samples to show the degree of reproducibility. All the pores have a length of 100 μm.

σ = 2.7 Å and ε = 230 K.[21] Following previous works on adsorption in porous gels or glasses, we neglect the interactions with the Al atoms of the substrate due to their low polarizability.[21] The Ar−O cross-parameters were calculated using the Lorentz−Berthelot mixing rules. The pore sizes in our molecular simulations are larger than those considered in the Experiment section. However, when giving the pore sizes in reduced unit with respect to the size of the fluid $D^* = D/\sigma$, one makes relevant the comparison between the experiments and molecular simulations. By doing this, a coarse-grained approach is adopted in which one considers the adsorption of a fluid particle of a size σ (i.e., a particle composed a large number of atoms or molecules) instead of the adsorption of single atoms or molecules. As previously noted by Woo and Monson,[22] such an approach allows considering large systems with reasonable computing time while capturing the physics of the mechanisms involved upon adsorption and desorption (but the details of the atomistic level are lost). In what follows, the pore sizes in the molecular simulations will be given in reduced units: $D^* = D/\sigma$ = 19 (6.4 nm) and 14 (4.8 nm).

Argon adsorption at 85 K in the atomistic models of porous anodized aluminum oxide was simulated by means of grand canonical Monte Carlo simulations.[23,24] The latter technique is a stochastic method that simulates a system having a constant volume V (the pore with the adsorbed phase), in equilibrium with an infinite reservoir of particles imposing its chemical potential μ and temperature T.[25−27] The absolute adsorption isotherm is given by the ensemble average of the number of adsorbed atoms as a function of the pressure of the gas reservoir P (the latter is obtained from the chemical potential μ according to the bulk equation of state for an ideal gas).[28] Periodic boundary conditions were used along the three directions x, y, z to avoid finite size effects.

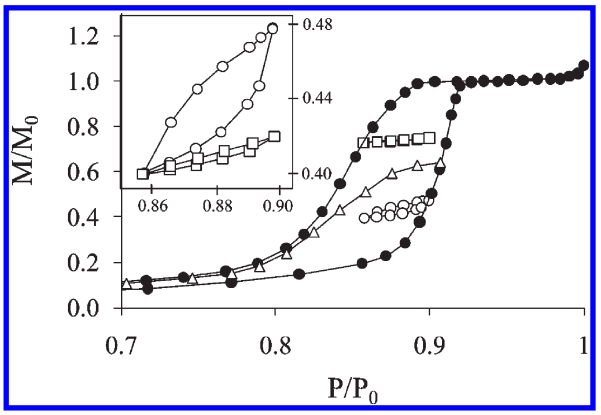

Figure 3. Experimental capillary condensation hysteresis loop for Ar in closed bottom pores with three modulations. A primary descending scanning curve and two subloops are also shown. The inset shows a comparison of the two subloops.

Results and Discussion

Figure 2 shows the experimental adsorption isotherms for argon at 85 K in modulated C pores (the same behavior has been observed with the modulated O pores). These curves show the adsorbed amounts M normalized to the total number of atoms, M_0, when the pores are filled, as a function of relative pressure, P/P_0, where P_0 = 65 kPa is the bulk saturating vapor pressure for Ar at 85 K. The isotherms for two samples with N = 20 have been plotted to show the degree of data reproducibility. As a useful reference, we have also displayed the isotherms in straight pores with D = 25 and 35 nm, which correspond to the diameters of the different sections of the modulated pores. All the curves show pronounced hysteresis loops between the condensation and evaporation branches. This observation is consistent with previous results obtained for porous silicon,[2,3,17] silicas,[29,30] and AAO.[6,31,32]

As expected, the condensation and evaporation pressures for the straight pores increase with D. According to Cohan's conjecture,[7] adsorption in C pores should be reversible. The hysteresis loops observed for the AAO with C pores, which are nearly identical to those found for the O pores, indicate the presence of morphological disorder within the pore. However, the fact that such hysteresis loops have nearly parallel adsorption and desorption branches (H1 type in the IUPAC classification[33]) suggests that the pore roughness is not as significant as in disordered materials like porous silicon that present asymmetrical hysteresis loops (H2 type). Actually, recent numerical studies[16,17] of adsorption in not connected model pores show that pore size disorder (i.e., variation of the pore size at the mesoscale) produces H1 type hysteresis loops regardless of the pores closure. If the pores are also rough (i.e., variation of the wall surface at the microscale), the hysteresis loop may exhibit H2 type hysteresis typical of three-dimensional networks like Vycor when the surface roughness affects the pore size distribution significantly.

Interestingly, the hysteresis loops for the modulated pores are almost superimposed. Furthermore, these loops are close to that obtained for the straight pores with D = 25 nm. This result suggests that the filling and emptying for the modulated pores are driven by the

(21) Brodka, A.; Zerda, T. W. *J. Chem. Phys.* **1991**, *95*, 3710–3718.
(22) Woo, H. J.; Porcheron, F.; Monson, P. A. *Langmuir* **2004**, *20*, 4743–4747.
(23) Coasne, B.; Alba-Simionesco, C.; Audonnet, F.; Dosseh, G.; Gubbins, K. E. *Langmuir* **2009**, *25*, 10648–10659.
(24) Coasne, B.; Di Renzo, F.; Galarneau, A.; Pellenq, R. J. M. *Langmuir* **2008**, *24*, 7285–7293.
(25) Nicholson, D.; Parsonage, N. G. *Computer Simulation and the Statistical Mechanics of Adsorption*; Academic Press: New York, 1982.
(26) Allen, M. P.; Tildesley, D. J. *Computer Simulation of Liquids*; Clarendon: Oxford, 1987.
(27) Frenkel, D.; Smit, B. *Understanding Molecular Simulation: From Algorithms to Applications*, 2nd ed.; Academic Press: London, 2002.
(28) Bhattacharya, S.; Coasne, B.; Hung, F. R.; Gubbins, K. E. *Langmuir* **2009**, *25*, 5802–5813.
(29) Grosman, A.; Ortega, C. *Langmuir* **2005**, *21*, 10515–10521.
(30) Esparza, J. M.; Ojeda, M. L.; Campero, A.; Dominguez, A.; Kornhauser, I.; Rojas, F.; Vidales, A. M.; Lopez, R. H.; Zgrablich, G. *Colloids Surf., A* **2004**, *241*, 35–45.
(31) Bruschi, L.; Fois, G.; Mistura, G.; Sklarek, K.; Hillebrand, R.; Steinhart, M.; Gosele, U. *Langmuir* **2008**, *24*, 10936–10941.
(32) Casanova, F.; Chiang, C. E.; Li, C. -P.; Roshchin, A.; Ruminski, M.; Sailor, J.; Schuller, I. K. *Europhys. Lett.* **2008**, *81*, 26003.
(33) Sing, K.; Everett, D.; Haul, R.; Moscou, L.; Pierotti, R.; Rouquerol, J.; Siemieniewska *Pure Appl. Chem.* **1985**, *57*, 603.

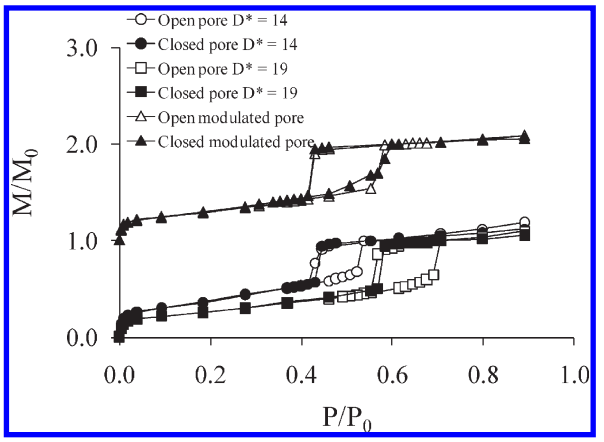

Figure 4. Simulated Ar adsorption isotherms at 85 K in regular and modulated AAO pores, opened at both ends and closed at one end. The curves for the modulated pores have been shifted up by +1 for the sake of clarity.

size of the smallest modulation. It also indicates the good uniformity of the AAO modulated pores. In fact, previous experiments with porous Si with an ink-bottle morphology of the pores found no difference in desorption irrespective of whether the bottle part has direct contact to the bulk phase or not.[3] According to recent simulations,[16,17] this is explained as the effect of very rough disordered pores which produce cavities in the pore body far away from the pore ends.

To better understand the origin of the hysteresis, we measured reversal curves and subloops in modulated porous AAO. Figure 3 shows the results for C pores with $N = 3$, which closely resemble those observed for straight pores.[31] First, the reversal curve, i.e., an adsorption curve obtained by decreasing the pressure starting from a point along the condensation branch, meets the desorption branch only at the closure of the loop. Moreover, the shapes of two subloops, i.e., two adsorption cycles obtained within the main hysteresis between the same pressure ends, are different. The same behavior was observed for open modulated pores. According to the independent domain theory by Everett,[8,34] both observations imply that the pores are not composed of independent domains but consists of an assembly of connected domains of different D.

The simulated adsorption isotherms for the regular cylindrical pores with $D^* = 14$ and $D^* = 19$ are shown in Figure 4. Both the results for C and O pores are reported. As for the experimental data, the simulated curves show the adsorbed amounts M normalized to the total number of atoms, M_0, when the pores are filled, as a function of relative pressure, P/P_0, where $P_0 = 65$ kPa is the bulk saturating vapor pressure for Ar at 85 K. We also show in Figure 5 molecular configurations upon adsorption and desorption in the nanopores with $D^* = 14$ (the same behavior is observed for the nanopore with $D^* = 19$). In all pores, the adsorbed amount is found to increase continuously until a jump occurs due to capillary condensation of the fluid. In agreement with the experiments above, the capillary condensation pressure increases with D. For the O pores, condensation occurs through an irreversible transition when the film adsorbed at the cylindrical pore surface becomes unstable while evaporation takes place through the displacement at equilibrium of a hemispherical meniscus along the pore axis. Instead, condensation in the C pores is continuous and reversible as the filling occurs through the displacement at equilibrium of a hemispherical meniscus along the pore axis. These results follow the predictions of Cohan's model and agree with previous simulations of adsorption and desorption in model pores of well-defined geometry.[10,11,35]

Figure 4 also shows the simulated argon adsorption isotherms for the modulated pores with open ends and with closed bottom ends. We also show in Figure 5 molecular configurations upon adsorption and desorption in these pores. The adsorption isotherms for the constricted O and C pores are nearly identical, in agreement with the experimental results reported above. The adsorbed amount increases continuously until a jump occurs at a pressure $P = 0.55P_0$ due to condensation in the constrictions. The filling mechanism of the constrictions is similar to that obtained for a regular pore. This is confirmed by the fact that the condensation pressure for these constrictions is very similar to that for the regular cylindrical nanopore having the same diameter, $P = 0.52P_0$. We note that the two values are slightly different because of finite size effects (finite length of the constriction). This difference is expected to vanish with increasing the length of the constriction as they would become close to ideal long cylindrical nanopores. (We note that the modulated/constricted parts in the experiments are very long as they are several micrometers long.) Moreover, given the uncertainty of a few $0.01P_0$ over the location of the condensation pressures, the latter two values can be considered as equal. Condensation in the constrictions leads to the formation of hemispherical gas/liquid interfaces (menisci) located in between the $D_c^* = 14$ constrictions and the $D^* = 19$ cavities. The filling of the remaining porosity (i.e., large cavities) occurs spontaneously once the constrictions are filled; this result is due to the fact that the size difference between the constriction and cavity (a ratio 2/3) is not large enough to observe different condensation pressures. In fact, the hemispherical menisci at the entrance of the large cavity (which appear once the constrictions are filled) impose that the pore filling in this large cavity occurs at equilibrium. If the cavity size is small enough, the at-equilibrium condensation pressure in the large cavity may be smaller than the metastable condensation pressure of the constriction so that condensation occurs as soon as the constrictions get filled. The evaporation pressure $P = 0.42P_0$ for the constricted O and C pores is much lower than the condensation pressure, so that a wide hysteresis loop is observed. In agreement with the experiments above, the evaporation pressures for the modulated pores are closed to that obtained for a regular cylindrical nanopore having the same diameter as the constrictions, $P = 0.40P_0$. This result suggests that desorption in the constricted nanopores occurs through pore blocking; i.e., evaporation in the large cavities is triggered by evaporation at equilibrium of the fluid in the constrictions.[16,17] Such a hypothesis is confirmed by the configurations obtained upon desorption; the fluid in the 6.4 nm cavities remains stable until evaporation in the constrictions occurs. The results above depart from what was reported in the pioneering work by Sarkisov and Monson on adsorption and condensation in ink-bottle pores.[10] These authors found that desorption in the large cavity occurs through cavitation, i.e., nucleation of the gas phase while the constriction remains filled by the liquid. As noted in refs 14 and 36, the observation of pore blocking or cavitation depends on the relative stability of the liquid confined in the constriction and that confined in the cavity. Starting with a completely filled pore, the liquid trapped in a cavity isolated from the gas phase through a filled constriction experiences a depression as the pressure decreases. Pore blocking is observed if the liquid in the cavity

(34) Coasne, B.; Gubbins, K. E.; Pellenq, R. J. M. *Phys. Rev. B* **2005**, *72*, 024304.
(35) Bohlen, H.; Parry, A. O.; Diaz-Herrera, E.; Schoen, M. *Langmuir* **2008**, *25*, 103.
(36) Coasne, B.; Gubbins, K. E.; Pellenq, R. J. M. *Part. Part. Syst. Charact.* **2004**, *21*, 149.

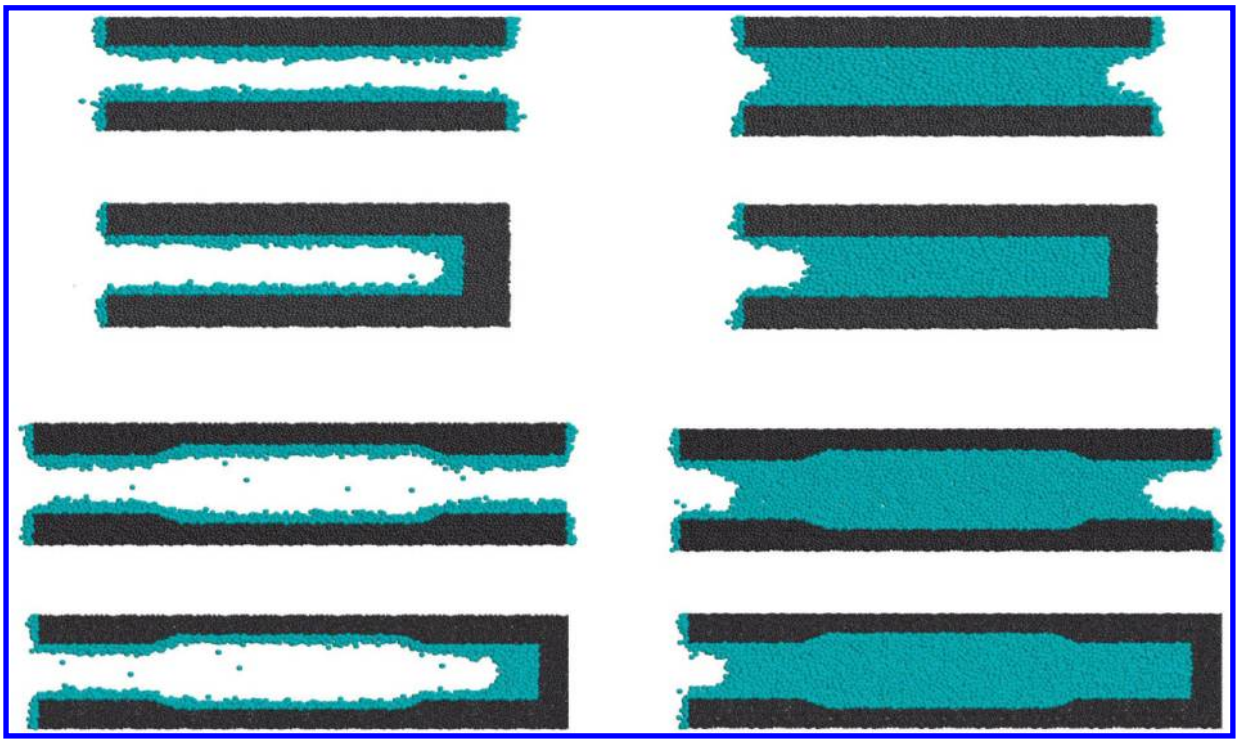

Figure 5. Typical molecular configurations for Ar adsorbed at 85 K in regular and modulated pores. Both pores open at both ends and closed at one end are shown. Cyan spheres are the Ar atoms and gray spheres the O atoms of the AAO pores.

can resist such a depression until the liquid in the constriction evaporates. In that case, the desorption of the liquid located in the constriction spontaneously triggers the evaporation of the liquid cavity (the latter being already at a pressure below its equilibrium pressure). On the other hand, cavitation is observed if the liquid in the cavity cannot resist the depression until the liquid in the constriction evaporates. In that case, the desorption of the liquid located in the constriction occurs through the spontaneous nucleation of a gas bubble, although the constriction remains filled by the liquid.

Conclusion

The experiments and molecular simulations reported in the present article provides interesting insights into condensation and evaporation in modulated nanopores where the surface roughness is much smaller than the difference between the size of the constrictions and that of the large sections. Both sets of data show that the adsorption in modulated pores exhibits pronounced hysteresis loops regardless of the pore openings. This result is due to the fact that capillary condensation and evaporation in these pores occur through the same filling and emptying mechanisms, which are driven by the smallest size of the nanopores. More generally, our results show that the adsorption and condensation mechanisms are greatly affected by the presence of the constrictions/modulations. Namely, the adsorption isotherm for the closed bottom pore with constrictions is irreversible while it should be reversible when the pore does not present any morphological defect. This confirms what was found in much more irregular linear pores.[5,16,17] An important result of the present study is that the adsorption isotherms are almost identical if constrictions are added to straight pore systems, regardless of their ending. This suggests that the hysteresis loops observed in closed bottom end AAO nanopores[6,31,32] are likely caused by variations in pore size along the pore axis. If the pores are somewhat disordered, we can explain the hysteresis found in open and closed pores because Cohan's argument applies only to regular cylindrical pores. We note that an analogous explanation based on such morphological inhomogeneities or "surface quenched disorder" has been suggested in the particular case of closed pores of porous silicon for which wide and asymmetric hysteresis loops are observed.[2,3,17] Finally, these results contribute to provide a general picture of capillary condensation and evaporation in constricted or modulated pores that can be used for the interpretation of adsorption in disordered porous materials.

Acknowledgment. We thank Francesco Ancilotto for clarifying comments. This work has been partially supported by Padua University through Project No. CPDA077281/07. We thank the French National Research Agency (ANR) for funding through the research project "SIMONANOMEM" (ANR-07-NANO-055-04). Calculations were performed using supercomputers at the Institut de Développement et des Ressources en Informatique Scientifique (IDRIS, CNRS, Grant No. 96223).